

1 **February 12, 2020:**

2 **Metabolic flexibility allows generalist bacteria**
3 **to become dominant in a frequently disturbed**
4 **ecosystem**

5 **Ya-Jou Chen^{1,2}, Pok Man Leung^{1,2}, Sean K. Bay^{1,2}, Philip Hugenholtz³, Adam J.**
6 **Kessler^{4,5}, Guy Shelley¹, David W. Waite^{3,6}, Perran L. M. Cook^{4*}, Chris**
7 **Greening^{1,2*}**

8

9 ¹ School of Biological Sciences, Monash University, Clayton, VIC 3800, Australia

10 ² Department of Microbiology, Biomedicine Discovery Institute, Clayton, VIC 3800,
11 Australia

12 ³ Australian Centre for Ecogenomics, School of Chemistry and Molecular Biosciences,
13 The University of Queensland, St Lucia, QLD 4072, Australia

14 ⁴ Water Studies Centre, School of Chemistry, Monash University, Clayton, VIC 3800,
15 Australia

16 ⁵ School of Earth, Atmosphere and Environment, Monash University, Clayton, VIC
17 3800, Australia

18 ⁶ School of Biological Sciences, University of Auckland, Auckland 1010, New Zealand

19

20 * Correspondence can be addressed to:

21

22 A/Prof Chris Greening (chris.greening@monash.edu)

23 Prof Perran Cook (perran.cook@monash.edu)

24

25 **Abstract**

26 Ecological theory suggests that habitat disturbance differentially influences
27 distributions of generalist and specialist species. While well-established for
28 macroorganisms, this theory has rarely been explored for microorganisms. Here we
29 tested these principles in permeable (sandy) sediments, ecosystems with much
30 spatiotemporal variation in resource availability and other conditions. Microbial
31 community composition and function was profiled in intertidal and subtidal sediments
32 using 16S amplicon sequencing and metagenomics, yielding 135 metagenome-
33 assembled genomes. Microbial abundance and composition significantly differed with
34 sediment depth and, to a lesser extent, sampling date. Several generalist taxa were
35 highly abundant and prevalent in all samples, including within orders Woeseiales and
36 Flavobacteriales; genome reconstructions indicate these facultatively anaerobic taxa
37 are highly metabolically flexible and adapt to fluctuations in resource availability by
38 using different electron donors and acceptors. In contrast, obligately anaerobic taxa
39 such as sulfate reducers (Desulfobacterales, Desulfobulbales) and proposed
40 candidate phylum MBNT15 were less abundant overall and only thrived in more stable
41 deeper sediments. We substantiated these findings by measuring three metabolic
42 processes in these sediments; whereas the generalist-associated processes of sulfide
43 oxidation and hydrogenogenic fermentation occurred rapidly at all depths, the
44 specialist-associated process of sulfate reduction was restricted to deeper sediments.
45 In addition, a manipulative experiment confirmed generalists outcompete specialist
46 taxa during simulated habitat disturbance. Altogether, these findings suggest that
47 metabolically flexible taxa become dominant in these highly dynamic environments,
48 whereas metabolic specialism restricts bacteria to narrower niches. Thus, an
49 ecological theory describing distribution patterns for macroorganisms likely extends to
50 microorganisms. Such findings have broad ecological and biogeochemical
51 ramifications.

52

53 Introduction

54 In macroecology, species are broadly classified as habitat generalists and specialists
55 depending on their niche breadth ^{1,2}. Both deterministic and stochastic factors control
56 the differential distributions of such species and in turn the maintenance of diversity ³.
57 With respect to deterministic factors, a pervasive ecological theory is that generalists
58 and specialists differ in performance traits, for example resource utilisation; it is
59 thought habitat generalists are more versatile but less efficient than habitat specialists,
60 whereas specialists perform fewer activities more effectively. By extension, it can be
61 predicted that specialists will outperform generalists in their optimal habitats, whereas
62 generalists will be favoured in environments with high spatial and temporal
63 heterogeneity ^{1,4}. In turn, there is evidence that both natural and anthropogenic habitat
64 disturbance favours generalists and promotes homogenisation of community
65 composition ⁵⁻⁷. Other factors, notably dispersal traits and life history strategies, also
66 influence distribution patterns ^{3,8}. While these tenets are well-established for animals
67 and plants, few studies have extended them to microbial communities ⁹⁻¹¹.

68
69 The key ecological processes governing macroorganism community assembly are
70 thought to extend to microorganisms. However, environmental filtering tends to
71 predominate over neutral factors such as dispersal limitation ¹²⁻¹⁴. In turn, these
72 processes lead to an uneven prevalence of microbial taxa across ecosystems; most
73 community members have low to intermediate occupancy (habitat specialists), but a
74 small proportion of taxa tend to be highly prevalent and often abundant across space
75 and time (habitat generalists) ^{15,16}. The performance traits that differentiate microbial
76 generalists and specialists have been scarcely explored. It is probable that, like
77 macroorganisms, a key factor that governs distribution patterns is the capacity and
78 efficiency of resource utilisation. In this regard, an important feature that distinguishes
79 microorganisms is their metabolic versatility ¹⁷; whereas plants and animals are
80 respectively restricted to photoautotrophic and chemoheterotrophic growth, many
81 microorganisms can use multiple energy sources, carbon sources, and oxidants either
82 simultaneously or alternately ¹¹. Likewise, the capacity for microorganisms to transition
83 between active and dormant states contributes to the maintenance of diversity ^{18,19}. It
84 is being increasingly realised that such flexibility in resource usage contributes to the
85 dominance of major taxa in various environments ²⁰⁻²⁴.

86

87 Permeable (sandy) sediments are ideal sites to explore the concepts of microbial
88 generalism and specialism. These ecosystems, spanning at least half the continental
89 shelf, are important regulators of oceanic biogeochemical cycling and primary
90 production^{25–27}. Their mixing layers are continuously disrupted as a result of porewater
91 advection, tidal flows, and other factors^{28–30}. As a result, resident microorganisms
92 experience large spatiotemporal variations in the availability of light, oxygen, and other
93 resources^{25,31}. In contrast, the microbial communities in the deeper sediment layers
94 are infrequently disturbed and are generally exposed to dark anoxic conditions³².
95 Despite these pressures, these sediments are known to harbour abundant, diverse,
96 and active microbial communities^{33–37}. Previous studies have indicated that there is a
97 rapid community turnover across depth and season in Wadden Sea sediments³³.
98 However, some lineages such as the Woeseiales appear to be abundant and
99 prevalent residents of all permeable sediments sampled worldwide^{21,38,39}. The
100 functional basis for their dominance is unclear. We have recently published evidence
101 that metabolic flexibility, including the ability of bacteria to shift from aerobic respiration
102 to hydrogenogenic fermentation in response to oxic-anoxic transitions, is an important
103 factor controlling the ecology and biogeochemistry of the communities in the mixing
104 layer^{38,40}.

105

106 In this study, we investigated the spatiotemporal distributions and metabolic traits of
107 habitat generalists and specialists in permeable sediments from Middle Park Beach,
108 Port Philip Bay, Australia. Given the above considerations, we hypothesised that the
109 mixing and deep layers of permeable sediments would select for different microbial
110 traits. The mixing layer, reflecting its spatiotemporal variability, would select for
111 microbial generalists with broad metabolic capabilities. In contrast, the less frequently
112 disturbed deep layer would select for relative specialists with restricted but efficient
113 anaerobic lifestyles. To test this, we used high-resolution community profiling to
114 determine the spatiotemporal distribution of bacterial and archaeal communities in
115 shallow, intermediate, and deep sediments. In combination, we used genome-
116 resolved metagenomics, biogeochemical assays, and perturbation experiments to
117 determine the metabolic capabilities of the most dominant habitat generalists and
118 specialists.

119

120 Results and Discussion

121

122 Habitat generalists dominate permeable sediments, but co-exist with depth- 123 restricted specialists

124

125 We used the 16S rRNA gene as a marker to profile the diversity, abundance, and
126 composition of the bacterial and archaeal communities in permeable sediments. 48
127 sand samples were profiled that were collected from intertidal and subtidal sediments
128 at three different depths (shallow: 0-3 cm, intermediate: 14-17 cm, deep: 27-30 cm)
129 and across eight different dates over the course of a year (**Table S1**). Alpha diversity
130 indices indicated that the sands support the co-existence of diverse microorganisms;
131 Shannon index was high across the samples (6.79 ± 0.30) and no significant
132 differences were observed across depth, zone, or time (**Fig. 1a, Fig. S1 & S2**).
133 However, a significant decrease in community abundance with depth (inferred from
134 16S rRNA gene copy number by qPCR) across the samples (**Fig. 1b**). This correlated
135 with the transition from the mixing zone (above 20 cm) to the sustained aphotic anoxic
136 zone (below 20 cm), as indicated by a sharp decrease in chlorophyll *a* abundance
137 (**Fig. 1c**) and an increase in acid-volatile sulfide concentrations (from below detection
138 limits to $0.16 \mu\text{mol g}^{-1}$).

139

140 Community profiling indicated that the sands harbour diverse communities dominated
141 by generalist taxa (**Table S1**). There was considerable variation in taxonomic
142 composition (**Fig. S3**) and beta diversity (**Fig. 1d**) across samples. These variations
143 were moderately correlated with sediment depth ($R^2 = 0.29$) and weakly correlated
144 with sampling date ($R^2 = 0.08$) (**Fig. 1d; Table S2**). Of the taxa (amplicon sequence
145 variants, ASVs) detected, most exhibited low to intermediate occupancy, i.e. they were
146 shared across several samples (**Fig. 1e & Fig. S4**). Consistent with the theory that
147 disturbance promotes community homogenisation, there was a higher number of
148 shared taxa in the shallow sands (average occupancy of 3.3 samples; 71 ASVs shared
149 across 15 samples) compared to deep sands (average occupancy of 2.3 samples; 0
150 ASVs shared across 15 samples). In line with previous observations³⁸, the most
151 abundant orders were Woeseiales ($10.3 \pm 4.7\%$) and Flavobacteriales ($10.9 \pm 5.1\%$),
152 both of which were detected across all samples. Various other taxa, notably within the

153 Pseudomonadales, Pirellulales, Microtrichales, Chitinophagales, and candidate
154 gammaproteobacterial order GCA.001735895, were also prevalent and abundant
155 **(Fig. 1f & Fig. S5)**. This suggests that these bacteria withstand large variations in
156 habitat composition and resource availability in these sands. These bacterial groups
157 were also the most abundant in metagenomes **(Table S3)**, based on community
158 profiling using conserved single-copy ribosomal protein genes **(Table S4 & Fig. S6)**.

159

160 Nevertheless, there was evidence of some environmentally-driven differentiation in
161 community composition. Community structure significantly differed between deep
162 sediments and those of the shallow and intermediate sediments in the mixing zone
163 **(Fig. 1d & Table S2)**, though overlapped at one sampling date. Consistently, the
164 abundance of several orders significantly increased with depth, notably
165 Desulfobacterales, Desulfobulbales, and Xanthomonadales **(Fig. 1f)**. Similarly, the
166 proposed candidate phylum MBNT15⁴¹ was 20-fold more abundant in deeper
167 samples based on amplicons **(Fig. 1f)** and metagenomes **(Fig. S5)**. This indicates that
168 that the anoxic conditions of these sediments have selected for expansion of
169 anaerobic specialists, including sulfate-reducing bacteria. However, read counts
170 greatly varied across sampling dates; for example, while Desulfobacterales and
171 Desulfobulbales attained relative abundances of 9% and 15% in the deep sediments,
172 they were absent from the sediments of the same depth in the last two sampling dates.
173 This indicates that these taxa, in contrast to the habitat generalists that they coexist
174 with, are relatively sensitive to the disturbance events (e.g. oxygenation) that still
175 occasionally affect deeper sediments. With respect to possible aerobic specialists, the
176 orders Chitinophagales and Rhodobacterales were significantly more abundant in
177 shallower sediments **(Fig. 1f)**. The latter order, which contains cultivated aerobic and
178 photosynthetic members⁴², is likely to thrive under oxic photic conditions and may
179 contribute to depth-related variations in chlorophyll *a* levels **(Fig. 1c)**.

180

181 **Metabolic flexibility differentiates habitat generalists and specialists**

182

183 We used genome-resolved metagenomics to gain an insight into the metabolic traits
184 of generalist and specialist community members. Sequencing, assembly, and binning
185 of metagenomes of intertidal and subtidal sands from each sediment depth **(Table S3**
186 **& S5)** yielded 38 high-quality and 97 medium-quality metagenome-assembled

187 genomes (MAGs) ⁴³ (**Table S6**). We additionally reanalyzed the 12 MAGs that we
188 previously reported from this study site ³⁸. Together, the resultant genomes span 13
189 phyla and 43 orders, including the most dominant taxa in the 16S profiles (**Fig. 1**). We
190 profiled the abundance of 44 marker genes in the short reads and derived genomes
191 to gain an insight into the metabolic capabilities of the generalist and specialist
192 community members (**Fig. 2**). This confirmed microbial communities within sands
193 adopt an extraordinary array of strategies for energy conservation.

194

195 Most community members are predicted to be aerobic heterotrophs capable of using
196 organic and inorganic energy sources. Based on short reads, most bacteria encoded
197 enzymes for sulfide and thiosulfate oxidation, i.e. sulfide-quinone oxidoreductase (Sqr,
198 53%), flavocytochrome *c* sulfide dehydrogenase (FCC, 12%), reverse dissimilatory
199 sulfite reductase (r-DsrA, 9%), and thiosulfohydrolase (SoxB, 16%) (**Fig. 2; Table S5**).
200 Concordantly, a similar proportion of the MAGs encoded these enzymes (**Fig. 2; Table**
201 **S6**) and phylogenetic trees confirmed all binned sequences affiliated with canonical
202 clades (**Fig. 3; Fig. S6 to S9**). Most Sqr sequences, including from Woeseiales,
203 Flavobacteriales, Rhodobacterales, and Microtrichales, affiliated with the type III clade
204 (**Fig. 3a**) known to support sulfide-dependent growth ^{44,45}. Also widespread were the
205 genes for consumption of carbon monoxide (CoxL, 19%; **Fig. S10**) and hydrogen gas
206 (group 1 and 2 [NiFe]-hydrogenases, 48%; **Fig. S11**). Most bacteria also appear to
207 have a large capacity to withstand variations in electron acceptor availability. In
208 addition to encoding terminal oxidases for aerobic respiration (**Fig. 2**), many are
209 predicted to mediate stepwise denitrification through nitrate (NarG and NapA, 49%;
210 **Fig. S12 & S13**), nitrite (NirS and NirK, 37%; **Fig. S14 & S15**), nitric oxide (NorB, 11%;
211 **Fig. S16**), and nitrous oxide (NosZ, 32%; **Fig. S17**), with fewer mediating dissimilatory
212 nitrate reduction to ammonium (DNRA *via* NrfA, 7%; **Fig. S18**) (**Fig. 2**). As we
213 previously reported ³⁸, hydrogenotrophic sulfur reduction (group 1e [NiFe]-
214 hydrogenases, 17%; **Fig. S11**) and facultative hydrogenogenic fermentation (group 3
215 [NiFe]-hydrogenases, 62%; **Fig. S19**) are also common. Diverse community members
216 were also capable of reducing other compounds (**Table S5**), such as ferric iron (MtrB,
217 20%; **Fig. S20**) and organohalides (RdhA, 21%; **Fig. S21**). By contrast, few are
218 predicted to mediate the specialist traits of ammonia, iron, nitrite, or methane
219 oxidation, methanogenesis, acetogenesis, and, in the mixing zone, sulfate reduction
220 (**Fig. 2; Table S5**).

221

222 Further analysis of the reconstructed genomes revealed that the most prevalent
223 members are highly metabolically flexible (**Table S6 & Fig. 2**). The Woeseiaceae bins,
224 representing one of the most abundant and prevalent families in the sediments,
225 encode enzymes for aerobic heterotrophy, aerobic sulfide oxidation, hydrogenotrophic
226 sulfur reduction, denitrification, fumarate reduction (**Fig. S22**), iron reduction, and
227 hydrogenogenic fermentation. Flavobacteriaceae are similarly flexible, capable of
228 harnessing energy from organic carbon, sulfide, formate, carbon monoxide, and
229 sunlight via proteorhodopsin (**Fig. S23**), as well as switching between aerobic
230 respiration, anaerobic respiration, and fermentation. Other inferred generalists,
231 including within highly abundant orders Pseudomonadales, Pirellulales,
232 Microtrichales, Rhodothermales, and GCA-1735895 (**Fig. 1f**), are also predicted to be
233 able to use multiple energy sources and electron acceptors in these sediments (**Fig.**
234 **2**). Altogether, this suggests most community members can accommodate
235 environmental fluctuations in electron acceptor availability by switching between
236 different respiratory and fermentative processes. Moreover, they can take advantage
237 of a wide range of organic and inorganic energy sources that are likely to be abundant
238 in these sediments. While most of the bacteria in the sediments were predicted to be
239 flexible, we detected no alternative metabolic pathways across multiple near-complete
240 MAGs from the Sphingomadales and Verrucomicrobiales (**Table S6**); these bacteria
241 may be aerobic organotrophic specialists, in line with their higher relative abundance
242 in surface sands (**Fig. 1f**).

243

244 The metagenomes also provide insights into the metabolic capabilities of community
245 members with more restricted distributions (i.e. relative habitat specialists). Whereas
246 the relative abundance of many generalist-associated genes (e.g. sulfide oxidation)
247 did not change with depth, there was a significant fivefold increase in the relative
248 abundance ($p < 0.0001$) of the marker genes for dissimilatory sulfate reduction (DsrA)
249 (**Fig. 3c; Fig. S8**) and the Wood-Ljungdahl pathway (AcsB) in the metagenomes of
250 deep sands compared to shallow and intermediate sands (**Fig. S20**). This strongly
251 correlates with the increased abundance of sulfate-reducing bacteria from the orders
252 Desulfobulbales and Desulfobacterales at these depths (**Fig. 1f**) that encode these
253 genes (**Fig. 2**). These bacteria are likely able to thrive in this niche by coupling the
254 oxidation of fermentative endproducts hydrogen (*via* group 1b and 1c [NiFe]-

255 hydrogenases; **Fig. S11**) and acetate (through the oxidative Wood-Ljungdahl
256 pathway; **Fig. S24**) to sulfate reduction. As highlighted in the phylogenetic trees of
257 **Figure 3**, the genes for the inferred specialist process of sulfate reduction were far
258 less abundant and widespread than those for sulfide oxidation. These sulfate-reducing
259 orders nevertheless possess some respiratory flexibility, including the ability to use
260 nitrate (**Fig. S13**) and organohalides (**Fig. S21**), suggesting they can accommodate
261 some changes in resource availability. However, in contrast to the facultative
262 anaerobes that they coexist with, these obligate anaerobes are expected to be
263 inhibited by oxygen given their terminal oxidases (**Fig. 2**) support detoxification rather
264 than growth. Similarly, genome reconstructions indicate MBNT15 bacteria are obligate
265 anaerobes that couple H₂ and acetate oxidation to nitrate reduction. Thus, these
266 lineages of Desulfobacterales, Desulfobulbales, and MBNT15 appear to be relative
267 habitat specialists that thrive in anoxic deep sediments, but lack the metabolic capacity
268 to compete in transiently oxygenated surface sediments.

269

270 **Metabolic processes associated with generalists and specialists show depth** 271 **variations in permeable sediments**

272

273 The above findings suggest that several alternative metabolic pathways, such as
274 sulfide oxidation and hydrogenogenic fermentation, allow habitat generalists to adapt
275 to changes in resource availability. The relative abundance of community members
276 that mediate these processes, as well as the metabolic genes that they encode, is
277 similar across depth (**Fig. 1f & 2**). Thus, it can be expected that these processes occur
278 in both shallow and deep sediments. To test this, we first measured rates of sulfide
279 oxidation in sediments spiked with sodium sulfide under oxic conditions. Sulfide was
280 rapidly consumed in a first-order kinetic process to below detection limits in both
281 shallow and deep sediments (**Fig. 4c**). We also measured hydrogenogenic
282 fermentation in sands under anoxic conditions; glucose addition stimulated rapid
283 accumulation of molecular hydrogen to micromolar levels in both surface and deep
284 sands (**Fig. 4a**).

285

286 In contrast, the community and metagenome data indicate that sulfate reducers are
287 habitat specialists that preferentially reside in the deeper sediments. To verify this, we
288 measured rates of hydrogenotrophic sulfate reduction in anoxic H₂-supplemented

289 surface and deep sediments. As anticipated given the abundance of hydrogenotrophic
290 sulfate reducers (**Fig. 1f**) and *dsrA* genes (**Fig. 2**), the microbial communities in deep
291 sediments consumed most H₂ within 48 hours (**Fig. 4a**), concomitant with
292 accumulation of 10 µM sulfide (**Fig. 4b**). In contrast, in line with our recent previous
293 observations^{38,40}, fermentation and respiration became uncoupled in surface
294 sediments following the onset of anoxia; rates of fermentation initially exceeded
295 respiration, resulting in net H₂ accumulation and no detectable sulfide production
296 within 48 hours. Hydrogenotrophic sulfate reduction only became dominant after
297 prolonged incubations under anoxia (**Fig. 4a & 4b**), likely due to growth of sulfate-
298 reducing bacteria under these stable conditions.

299

300 **Metabolically flexible bacteria outcompete specialists during simulated** 301 **disturbance events**

302

303 The above insights from community, metagenomic, and biogeochemical profiling
304 suggest that metabolic flexibility facilitates habitat generalism of microorganisms in
305 permeable sediments. We performed a manipulative incubation experiment to test
306 whether the above inferences are valid. Samples collected from shallow and deep
307 sediments were incubated for 14 days under one of three conditions: continual light
308 oxic conditions, continual dark anoxic conditions, and disturbed conditions (24-hour
309 cycles between light oxic and dark anoxic conditions). Changes in the relative
310 abundance of key orders previously highlighted in the community (**Fig. 1**) and
311 metagenome (**Fig. 2**) analyses are shown in **Fig. 5**.

312

313 Most orders predicted to be metabolically flexible were able to tolerate being incubated
314 under all three conditions. These inferred generalists were dominant in all samples,
315 with highest relative abundances compared to inferred specialists in the original
316 samples and disturbed incubations (**Fig. 5**). Reflecting this, there were relatively minor
317 changes in the relative abundance of Woeseiales, Microtrichales, Rhodothermales,
318 and GCA_1735895 between time of sampling and following two weeks of incubations.
319 We also monitored the patterns of lineages predicted to be aerobic specialists
320 (Verrucomicrobiales, Sphingomondales) and anaerobic specialists
321 (Desulfobacterales, Desulfobulbales, Bacteroidales) based on the reconstructed
322 genomes (**Fig. 2**). Consistent with expectations, the relative abundance of both groups

323 declined by 40% in the disturbed slurries compared to the original samples. The
324 inferred aerobic specialists, while always relatively minor community members, were
325 most abundant in oxic incubations (4.7%) and least in anoxic sediments (2.1%).
326 Inferred anoxic specialists showed the reciprocal pattern. They bloomed to one third
327 of the community in the anoxic incubations (30%), but declined during oxygen
328 exposure (8%) (**Fig. 5**). It is likely that, under stable anoxic conditions, these anaerobic
329 specialists rapidly mobilize available resources through their sulfate reduction and
330 fermentation pathways.

331

332 Remarkably, some taxa thrived in response to disturbance. Flavobacteriales sampled
333 from deep sediments increased in relative abundance by 2.5-fold in the disturbed
334 incubations (**Fig. 5**), largely driven by expansions of genus *Eudoraea* (**Table S7**).
335 Based on the metabolic capabilities of the three MAGs from this genus (**Table S6**), it
336 is possible such bacteria take advantage of necromass released during oxic-anoxic
337 transitions by switching between aerobic respiration and hydrogenogenic fermentation
338 pathways. Likewise, there were significant enrichments in the two dominant groups of
339 phototrophs in the sediments, namely Rhodobacterales and diatoms (detected by
340 chloroplast 16S sequences) (**Fig. 1f & Table S5**). These taxa likely benefit from the
341 increased light availability under both the light oxic and disturbed conditions compared
342 to natural sediments, but must also possess sufficient metabolic flexibility to persist
343 under dark anoxic conditions; such flexibility is apparent from the diverse repertoire of
344 Rhodobacterales MAGs (**Fig. 2**), as well as previous studies inferring diatoms survive
345 dark anoxic conditions through nitrate respiration⁴⁶ and microbiota-mediated
346 hydrogenogenic fermentation^{38,40}. Although this experiment generally substantiated
347 metagenome-based inferences, a few taxa behaved contrary to predictions. Most
348 notably, Chitinophagales significantly decreased under anoxic conditions despite
349 harbouring genes for hydrogenogenic fermentation (**Fig. S18**), suggesting members
350 of this order either cannot survive in these conditions or are outcompeted by more
351 efficient anaerobes; these observations are nevertheless consistent with the
352 significant decrease in the relative abundance of this order with depth (**Fig. 1f**).

353

354 **Broader ecological and biogeochemical significance of findings**

355

356 In combination, these results provide multifaceted evidence that environmental
357 disturbance influences distributions of microbial habitat generalists and specialists.
358 The microbial communities in the mixing zone of permeable sediments experience
359 frequent but irregular spatiotemporal variations in oxygen, sunlight, nutrients, and
360 redox state ²⁵. Based on ecological theory, it would be expected that these variations
361 would differentially affect generalists and specialists ^{1,4}. For the specialists, these
362 changes would promote continual cycles of growth and death as conditions alternate
363 between favourable and unfavourable. In contrast, generalists are expected to
364 maintain more stable populations given they are more adaptable to environmental
365 change. We observed that habitat generalists are indeed more competitive in these
366 environments. Large and stable populations of taxa such as Woeseiales,
367 Flavobacteriales, and Pseudomonadales were present in both the mixing and deep
368 layers of the sampled sediments across sampling times, and were enriched under
369 simulated disturbance conditions in the manipulative incubations. Thus, in line with
370 observations for macroorganisms, environmental disturbance appears to promote
371 homogenisation of microbial community composition.

372

373 Some relative habitat specialists nevertheless coexist with such generalists in these
374 environments. Numerous taxa were detected with low occupancies and abundances,
375 several of which bloomed under favourable conditions, most notably MBNT15. The
376 manipulative incubation experiments confirmed that these inferred specialists only
377 became enriched under more stable conditions (light oxic for aerobes, dark anoxic for
378 anaerobes). Most notably, Desulfobacterales were the most abundant order in deep
379 sediments at certain sampling times and during prolonged dark anoxic incubations,
380 reflecting that sulfate-reducing bacteria thrive in stable hydrogen- and sulfate-rich
381 environments. These taxa and other anaerobic specialists nevertheless exhibited
382 sharp variations in relative abundance across the sampling dates, as well as significant
383 declines under oxic and disturbed incubations. In line with ecological paradigms, this
384 suggests that such specialists are highly sensitive to the disturbances that define the
385 mixing zone and occasionally affect deeper sands, whereas the generalists that they
386 coexist with are more adaptable. More data is required across various spatial and
387 temporal scales to ultimately understand the physicochemical pressures and
388 biological interactions that drive these differences. However, it is probable that oxygen
389 availability is the most significant factor that regulates composition, for example

390 through causing poisoning or promoting outcompetition by generalists better adapted
391 to these conditions ³⁸.

392

393 In turn, our study lends strong support to the hypothesis that microbial habitat
394 generalists and specialists have distinct metabolic capabilities. Based on the
395 reconstructed genomes, the generalists in the community are predicted to be
396 extremely metabolically flexible. Most notably, the Woeseiaceae that dominate these
397 sands are among the most flexible microorganisms ever described, given they are
398 predicted to use wide spectrum of electron donors (organic carbon, sulfide, hydrogen),
399 oxidants (oxygen, nitrite, fumarate, sulfur, fermentation), and based on previous
400 analysis ²¹, carbon sources (heterotrophy, autotrophy). Flavobacteriaceae have
401 similar metabolic breadth, likely underlying their expansion in response to disturbance.
402 By contrast, relative habitat specialists from the Desulfobacterales and
403 Desulfobulbales are distinguished by their capacity to use the abundant electron
404 acceptor sulfate, but also their inability to grow by aerobic respiration. These bacteria
405 possess some metabolic flexibility, likely explaining why these orders were detected
406 in low levels even in most surface sediments and oxygenated slurries; indeed, habitat
407 generalism and metabolic flexibility alike should be considered as continuous traits.
408 However, such obligate anaerobes are outcompeted by facultative anaerobes under
409 disturbed conditions. These inferred differences were strongly supported by
410 biogeochemical assays showing that, whereas sulfate reduction is limited to sediments
411 under prolonged anoxia, metabolic traits associated with generalists are active through
412 sediment zones. Further culture-dependent and culture-independent work, however,
413 is required to comprehensively understand the metabolic capabilities of permeable
414 sediment bacteria and their responses to environmental changes.

415

416 These findings also have important implications for how we conceive and model
417 biogeochemical processes. Models describing these processes can either take an
418 organism-centric approach or a systems perspective ⁴⁷. In the first case, the presence
419 or absence of a particular organism will determine the process taking place and
420 emphasis is placed on modelling the growth of that organism. In the second case,
421 thermodynamics and physical conditions determine the processes taking place.
422 Biogeochemists typically use the second approach to successfully predict and model
423 sediment processes ⁴⁸. Under conditions of continual disturbance, we show that

424 generalists dominate, and the energy conservation pathways that are used
425 (particularly under anaerobic conditions) will not be those predicted from
426 thermodynamics until specialists dominate (such as sulfate reduction). Under
427 disturbed conditions, therefore, community structure and the presence of generalists
428 (the organism-centric view) becomes an important consideration for predicting
429 ecosystem processes. Consistent with this, it has been shown that physicochemical
430 variables are strongest predictor of microbially driven ecosystem processes, but that
431 microbial community structure can improve these predictions in some cases ⁴⁹. Future
432 studies should incorporate disturbance as a co-variate when comparing the efficacy
433 of organism and system scale models (both statistical and deterministic).

434

435 In combination, we conclude that habitat generalists thrive in the disturbed
436 environments of permeable sediments and generally outcompete specialists. This
437 reflects their greater metabolic flexibility, particularly their capacity to shift between
438 electron acceptors during oxic-anoxic transitions. Relative habitat specialists have
439 narrower niches, but are highly competitive under more stable conditions. These
440 findings are substantiated through community and metagenomic profiling,
441 biogeochemical measurements, and manipulative experiments. Thus, a long-standing
442 ecological theory explaining differential distribution patterns of macroorganisms
443 appears to extend to microorganisms and we provide a mechanistic rationale for these
444 observations. Though further studies are required to extend these findings beyond
445 permeable sediments, it is probable that metabolic flexibility is a key factor governing
446 distributions of generalist and specialist taxa across ecosystems.

447

448 **Materials and Methods**

449

450 **Sampling of permeable sediments**

451 Permeable sediments were sampled from Middle Park Beach, Port Phillip Bay,
452 Sediments for microbial community profiling were collected over eight different
453 sampling dates over the course of a year (A: 28/10/2016; B: 13/12/2016; C: 19/1/2017;
454 D: 28/3/2017; E: 9/5/2017; F: 30/6/2017; G: 23/8/2017; H: 19/10/2017). Cores of 30
455 cm were used to collect sediments from the subtidal zone (~1 m deep at low tide) and
456 intertidal zone (~1 m deep at high tide). Cores were kept on ice until delivery to the

457 laboratory and were then immediately sectioned into shallow (0-3 cm), intermediate
458 (14-17 cm), and deep (27-30 cm) samples. All samples were subsequently stored at -
459 20°C until further processing.

460

461 **Amplicon sequencing**

462 For amplicon sequencing, total community DNA was extracted from 0.25 g of sediment
463 using the modified Griffith's protocol ⁵⁰. The yield, purity, and integrity of DNA from
464 each extraction was confirmed using a Qubit Fluorometer, Nanodrop 1000
465 Spectrophotometer, and agarose gel electrophoresis. For each sample, the V4
466 hypervariable region for 16S rRNA gene was amplified using the universal Earth
467 Microbiome Project primer pairs F515 and R806 ⁵¹ and subjected to Illumina paired-
468 end sequencing at the Australian Centre for Ecogenomics, University of Queensland.
469 Paired-end raw reads were demultiplexed and adapter sequences were trimmed,
470 yielding 1,362,535 reads across all samples. Forward and reverse sequences were
471 merged using the q2-vsearch plugin ⁵². A quality filtering step was applied using a
472 sliding window of four bases with an average base call accuracy of 99% (Phred score
473 20). The reads were truncated down to 250 base pairs to remove low quality reads
474 before de-noising using the deblur pipeline ⁵³ in QIIME 2 ⁵⁴. Samples with read counts
475 less than 1000 were removed from the further analysis. A total of 42 samples remained
476 after removing six samples. Amplicon sequence variants (ASVs) occurring once were
477 removed from the dataset. A total of 12,566 ASVs remained after removing 270
478 singletons. For taxonomic assignment, all reference reads that matched the
479 F515/R806 primer pair were extracted from the Genome Taxonomy Database (GTDB)
480 ⁴¹ and used to train a naïve bayes classifier by using the fit-classifier-naive-bayes
481 function with default parameters.

482

483 **Biodiversity analysis**

484 All statistical analysis and visualizations were performed with R software version 3.5.0
485 (April 2018) using the packages phyloseq ⁵⁵, vegan ⁵⁶, and ggplot2 ⁵⁷. Prior to
486 statistical analysis, all sequences were rarefied at 5,000 sequences per sample. Alpha
487 diversity was calculated using several metrics, including Shannon index, which
488 measures both species richness and evenness. We tested for significant differences
489 in Shannon index between depth, tidal zone, and date using an ANOVA (one-way
490 analysis of variance) with Tukey's *post hoc* tests ($p < 0.05$). Beta diversity was

491 calculated using weighted UniFrac distances⁵⁸ of log₁₀-transformed data and
492 visualized using principal coordinate analysis (PCoA). A pairwise analysis of
493 similarities (ANOSIM) was used to test for significant differences in community
494 similarity between depths, tidal zone, and date. First, permutational multivariate
495 analysis of variance (PERMANOVA) was performed using 999 permutations to test
496 for significant differences. Second, a beta dispersion test (PERMDISP) was used to
497 ascertain if observed differences were influenced by dispersion.

498

499 **Quantitative PCR**

500 Quantitative PCR (qPCR) was used to absolutely quantify the copy number of the 16S
501 rRNA genes in the samples. Amplifications were performed using a 96-well plate in a
502 pre-heated LightCycler® 480 Instrument II (Roche, Basel, Switzerland). Each well
503 contained a 10 µl reaction mixture comprising 1 µl DNA template, 5 µl PlatinumT
504 SYBRGreen qPCR SuperMix-UDG with ROX, 0.5 µl each of the universal 16S rRNA
505 gene V4 primers F515 and R806 (10 µM)⁵¹, and 3 µl UltraPure Water (Thermo Fisher
506 Scientific, Waltham, MA, USA). Each amplification was performed in technical
507 triplicate. Cycling conditions were as follows: 3 min denaturation at 94°C followed by
508 40 cycles of 45 s denaturation at 94°C, 60 s annealing at 50°C, and 90 s extension at
509 72°C. Copy number was quantified against a pMA vector standard containing a single
510 copy of the *Escherichia coli* 16S rRNA gene. Dilutions ranged from 10³ to 10⁸ copies
511 µl⁻¹ and the qPCR amplification efficiency ranged from 85-94% (R² > 0.99).

512

513 **Chlorophyll a measurements**

514 Chlorophyll a was extracted using a previously described method⁵⁹. Briefly, 5 mL of
515 90% acetone (v/v) was added to 5 g of sediments in 50 ml Falcon tubes. Samples
516 were then stored overnight in the dark at 4°C. Subsequently, all samples were
517 subsequently centrifuged at 550 × g for 15 minutes and 3 mL of supernatant was
518 transferred into cuvettes. Chlorophyll absorbance was measured
519 spectrophotometrically using a Hitachi U-2800 spectrophotometer (Hitachi High-
520 Technologies Corporation, Tokyo, Japan) at five different wavelengths (630, 647, 664,
521 665, and 750 nm). Spectra were read before and after acidification with 10 µL of 1 M
522 HCl (v/v). After calculating the difference in absorbance between the first and second
523 measurement, chlorophyll a concentration was determined using the equation of
524 Lorenzen⁵⁹.

525

526 **Shotgun metagenome sequencing**

527 **Table S1** summarizes details of the metagenomic datasets. For this study, we
528 sequenced eight new metagenomes (subtidal deep A, intertidal deep A, subtidal
529 shallow C, intertidal shallow C, subtidal intermediate C, intertidal shallow C, subtidal
530 deep C, intertidal deep C) and analyzed five previously reported metagenomes
531 (subtidal shallow A, subtidal intermediate A, intertidal shallow A, intertidal intermediate
532 A, flow-through reactor)³⁸. DNA was extracted from the 0.3 g of sediment, collected
533 during the October 2016 (A samples) and January 2017 (C samples) field trips, using
534 the MoBio PowerSoil Isolation kit according to manufacturer's instructions.
535 Metagenomic shotgun libraries were prepared for each sample using the Nextera XT
536 DNA Sample Preparation Kit (Illumina Inc., San Diego, CA, USA) and sequencing was
537 performed on an Illumina NextSeq500 platform with a 2 × 150 bp High Output run.
538 Sequencing yielded 574,093,137 read pairs across the eight metagenomes. To
539 supplement the 16S amplicon sequencing data, community profiles in permeable
540 sediments were independently generated from metagenome reads that mapped to the
541 universal single copy ribosomal marker gene *rplP* using SingleM v.0.12.1 (
542 <https://github.com/wwood/singlem>)

543

544 **Shotgun metagenome assembly and binning**

545 The BBDuk function of the BBTools v38.51 (<https://sourceforge.net/projects/bbmap/>)
546 was used to clip contaminating adapters (k-mer size of 23 and hamming distance of
547 1), filter PhiX sequences (k-mer size of 31 and hamming distance of 1), and trim bases
548 with a Phred score below 20 from the raw metagenomes. 482,529,838 high-quality
549 read pairs with lengths over 50 bp were retained for downstream analysis. Reads were
550 assembled individually and collectively with MEGAHIT v1.2.9⁶⁰ (--k-min 27, --k-max
551 127, --k-step 10). Bowtie2 v2.3.5⁶¹ was used to map short reads back to assembled
552 contigs using default parameters to generate coverage profiles. Subsequently,
553 genomic binning was performed using CONCOCT v1.1.0⁶², MaxBin2 v2.2.6⁶³, and
554 MetaBAT2 v2.13⁶⁴ and bins from the same assembly were then dereplicated using
555 DAS_Tool v1.1⁶⁵. Spurious contigs with incongruent genomic and taxonomic
556 properties and 16S rRNA genes in the resulting bins were removed using RefineM
557 v0.0.25⁶⁶. Applying a threshold average nucleotide identity of 99%, bins from different
558 assemblies were consolidated to a non-redundant set of metagenome-assembled

559 genomes (MAGs) using dRep v2.3.2 ⁶⁷. Completeness and contamination of MAGs
560 were assessed using CheckM v1.1.2 ⁶⁸. In total, 38 high quality (completeness > 90%
561 and contamination < 5%) and 97 medium quality (completeness > 50% and
562 contamination < 10%) ⁴³ MAGs were recovered and their corresponding taxonomy
563 was assigned by GTDB-TK v1.0.2 ⁴¹. Open reading frames (ORFs) in MAGs were
564 predicted using Prodigal v2.6.3 metagenomic setting ⁶⁹.

565

566 **Shotgun metagenome functional analysis**

567 To estimate the metabolic capability of the sediment communities, metagenomes and
568 derived genomes were searched against custom protein databases of representative
569 metabolic marker genes using DIAMOND v.0.9.22 (query cover > 80%) ⁷⁰. Searches
570 were carried out using all quality-filtered unassembled reads with lengths over 140 bp.
571 In addition, we searched ORFs from the 135 MAGs retrieved from this study and 12
572 MAGs that were previously reported ³⁸. These genes are involved in sulfur cycling
573 (AsrA, FCC, Sqr, DsrA, Sor, SoxB), nitrogen cycling (AmoA, HzsA, NifH, NarG, NapA,
574 NirS, NirK, NrfA, NosZ, NxrA, NorB), iron cycling (Cyc2, OmcB), reductive
575 dehalogenation (RdhA), photosynthesis (PsaA, PsbA, energy-converting microbial
576 rhodopsin), methane cycling (McrA, MmoA, PmoA), hydrogen cycling (large subunit
577 of NiFe-, FeFe-, and Fe-hydrogenases), carbon monoxide oxidation (CoxL), succinate
578 oxidation (SdhA), fumarate reduction (FrdA), and acetogenesis (AcsB) ⁷¹⁻⁷³. Results
579 were further filtered based on an identity threshold of 50%, except for group 4 NiFe-
580 hydrogenases, FeFe-hydrogenases, CoxL, AmoA, and NxrA (all 60%), PsaA (80%),
581 and PsbA (70%). Subgroup classification of reads was based on the closest match to
582 the sequences in databases. The presence of an additional set of genes involved in
583 oxidative phosphorylation (AtpA), NADH oxidation (NuoF), aerobic respiration (CoxA,
584 CcoN, CyoA, CydA), formate oxidation (FdhA), arsenic cycling (ARO, ArsC), iron
585 cycling (MtrB), selenium cycling (YgfK) in MAGs and contig ORFs was screened by
586 hidden Markov models (HMM) ⁷⁴, with search cutoff scores as described previously ⁷⁵.
587 Resulting hits were manually inspected to remove false positives. The screening of
588 these genes in uinassembled reads was carried out using DIAMOND blastp algorithm
589 (using binned and contig hits as reference sequences) with a minimum percentage
590 identity of 60% (NuoF), 70% (AtpA, FdhA, ARO), or 50% (all other databases). Read
591 counts to each gene were normalized to reads per kilobase million (RPKM) by dividing
592 the actual read count by the total number of reads (in millions) and then dividing by

593 the gene length (in kilobases; based on average gene length in custom databases and
594 gene length of representative sequence in Swiss-Prot database for HMMs were used).
595 In order to estimate the gene abundance in the microbial community, high-quality
596 unassembled reads were also screened for the 14 universal single copy ribosomal
597 marker genes used in SingleM v.0.12.1 and PhyloSift ⁷⁶ by DIAMOND (query cover >
598 80%, bitscore > 40) and normalized as above. Subsequently, the average gene copy
599 number of a gene in the community can be calculated by dividing the read count for
600 the gene (in RPKM) by the geometric mean of the read count of the 14 universal single
601 copy ribosomal marker genes (in RPKM).

602

603 **Phylogenetic analysis**

604 Phylogenetic analysis was used to verify the presence of key metabolic genes in
605 permeable sediment MAGs and determine which lineages were present. Phylogenetic
606 trees were constructed for 18 genes involved in energy conservation: dissimilatory
607 sulfite reductase (DsrA), sulfide-quinone oxidoreductase (Sqr), flavocytochrome *c*
608 sulfide dehydrogenase (FCC), thiohydrolase (SoxB), acetyl-CoA synthase (AcsB),
609 carbon monoxide dehydrogenase (CoxL), group 1 [NiFe]-hydrogenases, group 3
610 [NiFe]-hydrogenases, two nitrate reductases (NarG, NapA), three nitrite reductases
611 (NirS, NirK, NrfA), nitric oxide reductase (NorB), nitrous oxide reductase (NosZ),
612 decaheme iron reductase (MtrB), reductive dehalogenase (RdhA), fumarate reductase
613 (FrdA), and energy-converting microbial rhodopsins. In all cases, protein sequences
614 retrieved from the MAGs by homology-based searches were aligned against a subset
615 of reference sequences from the custom protein databases using ClustalW ⁷⁷ in
616 MEGA7 ⁷⁸. Evolutionary relationships were visualized by constructing maximum-
617 likelihood phylogenetic trees; specifically, initial trees for the heuristic search were
618 obtained automatically by applying Neighbour-Join and BioNJ algorithms to a matrix
619 of pairwise distances estimated using a JTT model, and then selecting the topology
620 with superior log likelihood value. All residues were used and trees were bootstrapped
621 with 50 replicates.

622

623 **Biogeochemical experiments**

624 Slurry experiments were performed to investigate the functional capacity of surface
625 and deep sands. Each slurry comprised a 160 mL serum vial containing 30 g of sieved
626 sand (wet weight) and 70 mL of seawater (filtered on 0.45 µm Whatman membrane

627 filters). The serum vials were sealed with butyl rubber stoppers and Wheaton closed-
628 top seals. Anoxic slurries were used to measure hydrogenogenic fermentation and
629 sulfate reduction in shallow and deep sands collected on November 12, 2018. Briefly,
630 the slurries were purged with high-purity helium and the headspace was amended with
631 100 ppmv H₂. Glucose was added to a final concentration of 1 mM for the glucose
632 addition group. All vials were incubated on a shaker (100 rpm) at room temperature.
633 For H₂ measurements, a 2 mL subsample was collected from headspace every 24 h
634 and analysed by gas chromatography. For sulfide measurements, a total of 8 mL of
635 seawater was extracted from each slurry and filtered for spectrophotometric analysis.
636 Three independent slurries were performed per treatment. Oxidic slurries were used to
637 measure aerobic sulfide oxidation in shallow and deep sands collected on December
638 6, 2018. The serum vials were aerated with lab air and sodium sulfide (Na₂S·9H₂O)
639 was added to a final concentration of 500 µM. All vials were incubated on a shaker
640 (100 rpm) at room temperature. A total of 8 mL of seawater was extracted from each
641 slurry and filtered for spectrophotometric analysis. The autoclaved vial was used as
642 the control group to control for the photochemical oxidation of sulfide in aqueous
643 solution. The amount of biogenic sulfide oxidation that occurred between each
644 timepoint was determined by calculating the difference between the treatment and
645 control groups.

646

647 **Molecular hydrogen and sulfide measurements**

648 To measure molecular hydrogen (H₂), 2 mL gas samples extracted during the slurry
649 experiments were injected into a VICI Trace Gas Analyser (TGA) Model 6K (Valco
650 Instruments Co. Inc., USA) fitted with a pulsed discharge helium ionisation detector
651 (PDHID) as previously described⁷⁹. Ultra-pure helium (99.999% pure, AirLiquide) was
652 used as a carrier gas at a pressure of 90 psi. The temperatures of column A (HayeSep
653 DB), column B (Molesieve 5Å), and the detector were 55 °C, 140 °C and 100 °C
654 respectively. The instrument was calibrated using standards of ultra-pure H₂ (99.999%
655 pure, AirLiquide) in ultra-pure He. Sulfide concentrations were quantified through the
656 methylene blue method with GBC UV-Visible 918 Spectrophotometer at 670 nm as
657 previously described⁸⁰.

658

659 **Long-term incubation experiments**

660 A long-term incubation experiment was performed to compare how habitat stability
661 and variability affects the community structure of permeable sediments. Surface (0-3
662 cm) and deep (20-25 cm) sediments were collected from Middle Park beach on
663 October 9, 2019. They were incubated in slurries comprising a 160 mL serum vial
664 containing 30 g of sieved sand (wet weight) and 70 mL of seawater (filtered on 0.45
665 μm Whatman membrane filters). The vials were sealed with butyl rubber stoppers and
666 Wheaton closed-top seals. All vials were incubated on a shaker (100 rpm) at room
667 temperature. Three different treatments were applied for both surface and deep. For
668 the light oxic slurries, vials were aerated daily with laboratory air and continuously
669 exposed to $60 \mu\text{mol photons m}^{-2} \text{s}^{-1}$. For the dark anoxic slurries, vials were purged
670 with high-purity nitrogen gas and covered with aluminium foil. For the oxic-anoxic
671 transition slurries, vials were transferred between light oxic to dark anoxic conditions
672 every 24 hours. All incubations were performed in triplicate. DNA was extracted from
673 the original sediments (control group) and each slurry after 14 days of incubation.
674 Community structure was determined by 16S amplicon sequencing as described
675 above.

676

677 References

- 678 1. Wilson, D. S. & Yoshimura, J. On the coexistence of specialists and
679 generalists. *Am. Nat.* **144**, 692–707 (1994).
- 680 2. Slatyer, R. A., Hirst, M. & Sexton, J. P. Niche breadth predicts geographical
681 range size: a general ecological pattern. *Ecol. Lett.* **16**, 1104–1114 (2013).
- 682 3. Büchi, L. & Vuilleumier, S. Coexistence of specialist and generalist species is
683 shaped by dispersal and environmental factors. *Am. Nat.* **183**, 612–624
684 (2014).
- 685 4. Kassen, R. The experimental evolution of specialists, generalists, and the
686 maintenance of diversity. *J. Evol. Biol.* **15**, 173–190 (2002).
- 687 5. Devictor, V., Julliard, R. & Jiguet, F. Distribution of specialist and generalist
688 species along spatial gradients of habitat disturbance and fragmentation.
689 *Oikos* **117**, 507–514 (2008).
- 690 6. Clavel, J., Julliard, R. & Devictor, V. Worldwide decline of specialist species:
691 toward a global functional homogenization? *Front. Ecol. Environ.* **9**, 222–228
692 (2011).

- 693 7. Marvier, M., Kareiva, P. & Neubert, M. G. Habitat destruction, fragmentation,
694 and disturbance promote invasion by habitat generalists in a multispecies
695 metapopulation. *Risk Anal. An Int. J.* **24**, 869–878 (2004).
- 696 8. Loehle, C. Strategy space and the disturbance spectrum: a life-history model
697 for tree species coexistence. *Am. Nat.* **156**, 14–33 (2000).
- 698 9. Székely, A. J. & Langenheder, S. The importance of species sorting differs
699 between habitat generalists and specialists in bacterial communities. *FEMS*
700 *Microbiol. Ecol.* **87**, 102–112 (2014).
- 701 10. Mariadassou, M., Pichon, S. & Ebert, D. Microbial ecosystems are dominated
702 by specialist taxa. *Ecol. Lett.* **18**, 974–982 (2015).
- 703 11. Carbonero, F., Oakley, B. B. & Purdy, K. J. Metabolic flexibility as a major
704 predictor of spatial distribution in microbial communities. *PLoS One* **9**, e85105
705 (2014).
- 706 12. Nemergut, D. R. *et al.* Patterns and processes of microbial community
707 assembly. *Microbiol. Mol. Biol. Rev.* **77**, 342–356 (2013).
- 708 13. Wang, J. *et al.* Phylogenetic beta diversity in bacterial assemblages across
709 ecosystems: Deterministic versus stochastic processes. *ISME J.* **7**, 1310–1321
710 (2013).
- 711 14. Caruso, T. *et al.* Stochastic and deterministic processes interact in the
712 assembly of desert microbial communities on a global scale. *ISME J.* **5**, 1406
713 (2011).
- 714 15. Delgado-Baquerizo, M. *et al.* A global atlas of the dominant bacteria found in
715 soil. *Science* **359**, 320–325 (2018).
- 716 16. Sunagawa, S. *et al.* Structure and function of the global ocean microbiome.
717 *Science* **348**, 1261359 (2015).
- 718 17. Nicholls, D. G. & Ferguson, S. *Bioenergetics*. (Academic Press, 2013).
- 719 18. Jones, S. E. & Lennon, J. T. Dormancy contributes to the maintenance of
720 microbial diversity. *Proc. Natl. Acad. Sci.* **107**, 5881–5886 (2010).
- 721 19. Lennon, J. T. & Jones, S. E. Microbial seed banks: the ecological and
722 evolutionary implications of dormancy. *Nat. Rev. Microbiol.* **9**, 119–130 (2011).
- 723 20. Ji, M. *et al.* Atmospheric trace gases support primary production in Antarctic
724 desert surface soil. *Nature* **552**, 400–403 (2017).
- 725 21. Mußmann, M., Pjevac, P., Krüger, K. & Dykma, S. Genomic repertoire of the
726 Woeseiaceae/JTB255, cosmopolitan and abundant core members of microbial

- 727 communities in marine sediments. *ISME J.* **11**, 1276 (2017).
- 728 22. Tsementzi, D. *et al.* SAR11 bacteria linked to ocean anoxia and nitrogen loss.
729 *Nature* **536**, 179 (2016).
- 730 23. Carere, C. R. *et al.* Mixotrophy drives niche expansion of verrucomicrobial
731 methanotrophs. *ISME J* **11**, 2599–2610 (2017).
- 732 24. Greening, C., Grinter, R. & Chiri, E. Uncovering the metabolic strategies of the
733 dormant microbial majority: towards integrative approaches. *MSystems* **4**,
734 e00107-19 (2019).
- 735 25. Huettel, M., Berg, P. & Kostka, J. E. Benthic exchange and biogeochemical
736 cycling in permeable sediments. *Ann. Rev. Mar. Sci.* **6**, 23–51 (2014).
- 737 26. Boudreau, B. P. *et al.* Permeable marine sediments: overturning an old
738 paradigm. *EOS, Trans. Am. Geophys. Union* **82**, 133–136 (2001).
- 739 27. Devol, A. H. Denitrification, anammox, and N₂ production in marine sediments.
740 *Ann. Rev. Mar. Sci.* **7**, 403–423 (2015).
- 741 28. Reimers, C. E. *et al.* *In situ* measurements of advective solute transport in
742 permeable shelf sands. *Cont. Shelf Res.* **24**, 183–201 (2004).
- 743 29. Santos, I. R., Eyre, B. D. & Huettel, M. The driving forces of porewater and
744 groundwater flow in permeable coastal sediments: A review. *Estuar. Coast.*
745 *Shelf Sci.* **98**, 1–15 (2012).
- 746 30. Huettel, M., Ziebis, W. & Forster, S. Flow-induced uptake of particulate matter
747 in permeable sediments. *Limnol. Oceanogr.* **41**, 309–322 (1996).
- 748 31. Cook, P. L., Frank, W., Glud, R., Felix, J. & Markus, H. Benthic solute
749 exchange and carbon mineralization in two shallow subtidal sandy sediments:
750 Effect of advective pore-water exchange. *Limnol. Oceanogr.* **52**, 1943–1963
751 (2007).
- 752 32. Glud, R. N. Oxygen dynamics of marine sediments. *Mar. Biol. Res.* **4**, 243–289
753 (2008).
- 754 33. Gobet, A. *et al.* Diversity and dynamics of rare and of resident bacterial
755 populations in coastal sands. *ISME J.* **6**, 542 (2012).
- 756 34. Böer, S. I., Arnosti, C., Van Beusekom, J. E. E. & Boetius, A. Temporal
757 variations in microbial activities and carbon turnover in subtidal sandy
758 sediments. *Biogeosciences* **6**, 1149–1165 (2009).
- 759 35. Hunter, E. M., Mills, H. J. & Kostka, J. E. Microbial community diversity
760 associated with carbon and nitrogen cycling in permeable shelf sediments.

- 761 *Appl. Environ. Microbiol.* **72**, 5689–5701 (2006).
- 762 36. Probandt, D. *et al.* Permeability shapes bacterial communities in sublittoral
763 surface sediments. *Environ. Microbiol.* **19**, 1584–1599 (2017).
- 764 37. Probandt, D., Eickhorst, T., Ellrott, A., Amann, R. & Knittel, K. Microbial life on
765 a sand grain: from bulk sediment to single grains. *ISME J.* (2017).
- 766 38. Kessler, A. J. *et al.* Bacterial fermentation and respiration processes are
767 uncoupled in permeable sediments. *Nat. Microbiol.* **4**, 1014–1023 (2019).
- 768 39. Dyksma, S., Pjevac, P., Ovanesov, K. & Mussmann, M. Evidence for H₂
769 consumption by uncultured Desulfobacterales in coastal sediments. *Environ.*
770 *Microbiol.* **20**, 450–461 (2018).
- 771 40. Bourke, M. F. M. F. *et al.* Metabolism in anoxic permeable sediments is
772 dominated by eukaryotic dark fermentation. *Nat. Geosci.* **10**, 30–35 (2017).
- 773 41. Parks, D. H. *et al.* A standardized bacterial taxonomy based on genome
774 phylogeny substantially revises the tree of life. *Nat. Biotechnol.* **36**, 996–1004
775 (2018).
- 776 42. Pujalte, M. J., Lucena, T., Ruvira, M. A., Arahal, D. R. & Macián, M. C. The
777 family Rhodobacteraceae. in *The Prokaryotes: Alphaproteobacteria and*
778 *Betaproteobacteria* 439–512 (Springer, 2014).
- 779 43. Bowers, R. M. *et al.* Minimum information about a single amplified genome
780 (MISAG) and a metagenome-assembled genome (MIMAG) of bacteria and
781 archaea. *Nat. Biotechnol.* **35**, 725–731 (2017).
- 782 44. Lencina, A. M., Ding, Z., Schurig-Briccio, L. A. & Gennis, R. B.
783 Characterization of the type III sulfide: quinone oxidoreductase from *Caldivirga*
784 *maquilingensis* and its membrane binding. *Biochim. Biophys. Acta (BBA)-*
785 *Bioenergetics* **1827**, 266–275 (2013).
- 786 45. Han, Y. & Perner, M. Sulfide consumption in *Sulfurimonas denitrificans* and
787 heterologous expression of its three sulfide-quinone reductase homologs. *J.*
788 *Bacteriol.* **198**, 1260–1267 (2016).
- 789 46. Kamp, A., de Beer, D., Nitsch, J. L., Lavik, G. & Stief, P. Diatoms respire
790 nitrate to survive dark and anoxic conditions. *Proc. Natl. Acad. Sci.* **108**, 5649–
791 5654 (2011).
- 792 47. Algar, C. K. & Vallino, J. J. Predicting microbial nitrate reduction pathways in
793 coastal sediments. *Aquat. Microb. Ecol.* **71**, 223–238 (2014).
- 794 48. Canfield, D., Kristensen, E. & Thamdrup, B. *Aquatic geomicrobiology.*

- 795 (Elsevier, 2005).
- 796 49. Graham, E. B. *et al.* Microbes as engines of ecosystem function: when does
797 community structure enhance predictions of ecosystem processes? *Front.*
798 *Microbiol.* **7**, 214 (2016).
- 799 50. Paulin, M. M. *et al.* Improving Griffith's protocol for co-extraction of microbial
800 DNA and RNA in adsorptive soils. *Soil Biol. Biochem.* **63**, 37–49 (2013).
- 801 51. Caporaso, J. G. *et al.* Global patterns of 16S rRNA diversity at a depth of
802 millions of sequences per sample. *Proc. Natl. Acad. Sci.* **108**, 4516–4522
803 (2011).
- 804 52. Rognes, T., Flouri, T., Nichols, B., Quince, C. & Mahé, F. VSEARCH: a
805 versatile open source tool for metagenomics. *PeerJ* **4**, 2584 (2016).
- 806 53. Amir, A. *et al.* Deblur rapidly resolves single-nucleotide community sequence
807 patterns. *mSystems* **2**, e00191-16 (2017).
- 808 54. Bolyen, E. *et al.* Reproducible, interactive, scalable and extensible microbiome
809 data science using QIIME 2. *Nat. Biotechnol.* **37**, 852–857 (2019).
- 810 55. McMurdie, P. J. & Holmes, S. phyloseq: an R package for reproducible
811 interactive analysis and graphics of microbiome census data. *PLoS One* **8**,
812 e61217 (2013).
- 813 56. Oksanen, J. *et al.* Vegan: community ecology package. *R Packag. Version 2.*
814 *4-6* (2018).
- 815 57. Wickham, H. *ggplot2: elegant graphics for data analysis.* Springer (2016).
- 816 58. Lozupone, C., Lladser, M. E., Knights, D., Stombaugh, J. & Knight, R. UniFrac:
817 an effective distance metric for microbial community comparison. *ISME J.* **5**,
818 169 (2011).
- 819 59. Lorenzen, C. J. Determination of chlorophyll and pheo-pigments:
820 spectrophotometric equations 1. *Limnol. Oceanogr.* **12**, 343–346 (1967).
- 821 60. Li, D. H. *et al.* MEGAHIT v1.0: A fast and scalable metagenome assembler
822 driven by advanced methodologies and community practices. *Methods* **102**, 3–
823 11 (2016).
- 824 61. Langmead, B. & Salzberg, S. L. Fast gapped-read alignment with Bowtie 2.
825 *Nat. Methods* **9**, 357 (2012).
- 826 62. Alneberg, J. *et al.* Binning metagenomic contigs by coverage and composition.
827 *Nat. Methods* **11**, 1144 (2014).
- 828 63. Wu, Y.-W., Simmons, B. A. & Singer, S. W. MaxBin 2.0: an automated binning

- 829 algorithm to recover genomes from multiple metagenomic datasets.
830 *Bioinformatics* **32**, 605–607 (2015).
- 831 64. Kang, D. *et al.* MetaBAT 2: an adaptive binning algorithm for robust and
832 efficient genome reconstruction from metagenome assemblies. *PeerJ* **7**, e7359
833 (2019).
- 834 65. Sieber, C. M. K. *et al.* Recovery of genomes from metagenomes via a
835 dereplication, aggregation and scoring strategy. *Nat. Microbiol.* **1** (2018).
- 836 66. Parks, D. H. *et al.* Recovery of nearly 8,000 metagenome-assembled genomes
837 substantially expands the tree of life. *Nat. Microbiol.* **2**, 1533 (2017).
- 838 67. Olm, M. R., Brown, C. T., Brooks, B. & Banfield, J. F. dRep: a tool for fast and
839 accurate genomic comparisons that enables improved genome recovery from
840 metagenomes through de-replication. *ISME J.* **11**, 2864 (2017).
- 841 68. Parks, D. H., Imelfort, M., Skennerton, C. T., Hugenholtz, P. & Tyson, G. W.
842 CheckM: assessing the quality of microbial genomes recovered from isolates,
843 single cells, and metagenomes. *Genome Res.* **25**, 1043–1055 (2015).
- 844 69. Hyatt, D. *et al.* Prodigal: prokaryotic gene recognition and translation initiation
845 site identification. *BMC Bioinformatics* **11**, 119 (2010).
- 846 70. Buchfink, B., Xie, C. & Huson, D. H. Fast and sensitive protein alignment using
847 DIAMOND. *Nat. Methods* **12**, 59 (2014).
- 848 71. Greening, C. *et al.* Diverse hydrogen production and consumption pathways
849 influence methane production in ruminants. *ISME J.* **13**, 2617–2632 (2019).
- 850 72. Søndergaard, D., Pedersen, C. N. S. & Greening, C. HydDB: a web tool for
851 hydrogenase classification and analysis. *Sci. Rep.* **6**, 34212 (2016).
- 852 73. Cordero, P. R. F. *et al.* Atmospheric carbon monoxide oxidation is a
853 widespread mechanism supporting microbial survival. *ISME J.* **13**, 2868–2881
854 (2019).
- 855 74. Eddy, S. R. Accelerated profile HMM searches. *PLoS Comput. Biol.* **7**,
856 e1002195 (2011).
- 857 75. Anantharaman, K. *et al.* Thousands of microbial genomes shed light on
858 interconnected biogeochemical processes in an aquifer system. *Nat. Commun.*
859 **7**, 13219 (2016).
- 860 76. Darling, A. E. *et al.* PhyloSift: phylogenetic analysis of genomes and
861 metagenomes. *PeerJ* **2**, e243 (2014).
- 862 77. Larkin, M. A. *et al.* Clustal W and Clustal X version 2.0. *Bioinformatics* **23**,

863 2947–2948 (2007).

864 78. Kumar, S., Stecher, G. & Tamura, K. MEGA7: Molecular Evolutionary Genetics
865 Analysis version 7.0 for bigger datasets. *Mol. Biol. Evol.* msw054 (2016).

866 79. Islam, Z. F. *et al.* Two Chloroflexi classes independently evolved the ability to
867 persist on atmospheric hydrogen and carbon monoxide. *ISME J.* **13**, 1801–
868 1813 (2019).

869 80. Fonselius, S., Dyrssen, D. & Yhlen, B. Determination of hydrogen sulphide.
870 *Methods Seawater Anal. Third Ed.* 91–100 (2007).

871

872 **Footnotes**

873

874 **Data availability statement:** All amplicon sequencing data, raw metagenomes, and
875 metagenome-assembled genomes will be deposited to the Sequence Read Archive.

876

877 **Acknowledgements:** This study was supported by an ARC Discovery Project
878 (DP180101762; awarded to P.L.M.C. and C.G), an ARC DECRA Fellowship
879 (DE170100310; salary for C.G.), an ARC Laureate Fellowship (FL150100038;
880 awarded to P.H.), and an NHMRC EL2 Fellowship (APP1178715; salary for C.G.).
881 Y.J.C. was supported by PhD scholarships from Monash University and the Taiwan
882 Ministry of Education. We thank Dustin Marshall and Kim Handley for helpful
883 discussions, Rachael Lappan for providing R scripts, and Thanavit Jirapanjawat, David
884 Brehm, Vera Eate, Sharlynn Koh, Tess Hutchinson, and Zahra Islam for technical and
885 field assistance.

886

887 **Author contributions:** C.G. and P.L.M.C. conceived, designed, and supervised this
888 study. Y.-J.C. designed experiments, performed all field and laboratory work, and
889 analyzed data. P.M.L., C.G., D.J.W., and P.H. analysed metagenomes. G.S. and
890 S.K.B. provided experimental and analytical support. A.J.K. contributed to
891 conceptualisation, analysis, and interpretation. Y.-J.C. and C.G. wrote the paper with
892 input from all authors.

893

894 The authors declare no conflict of interest.

895

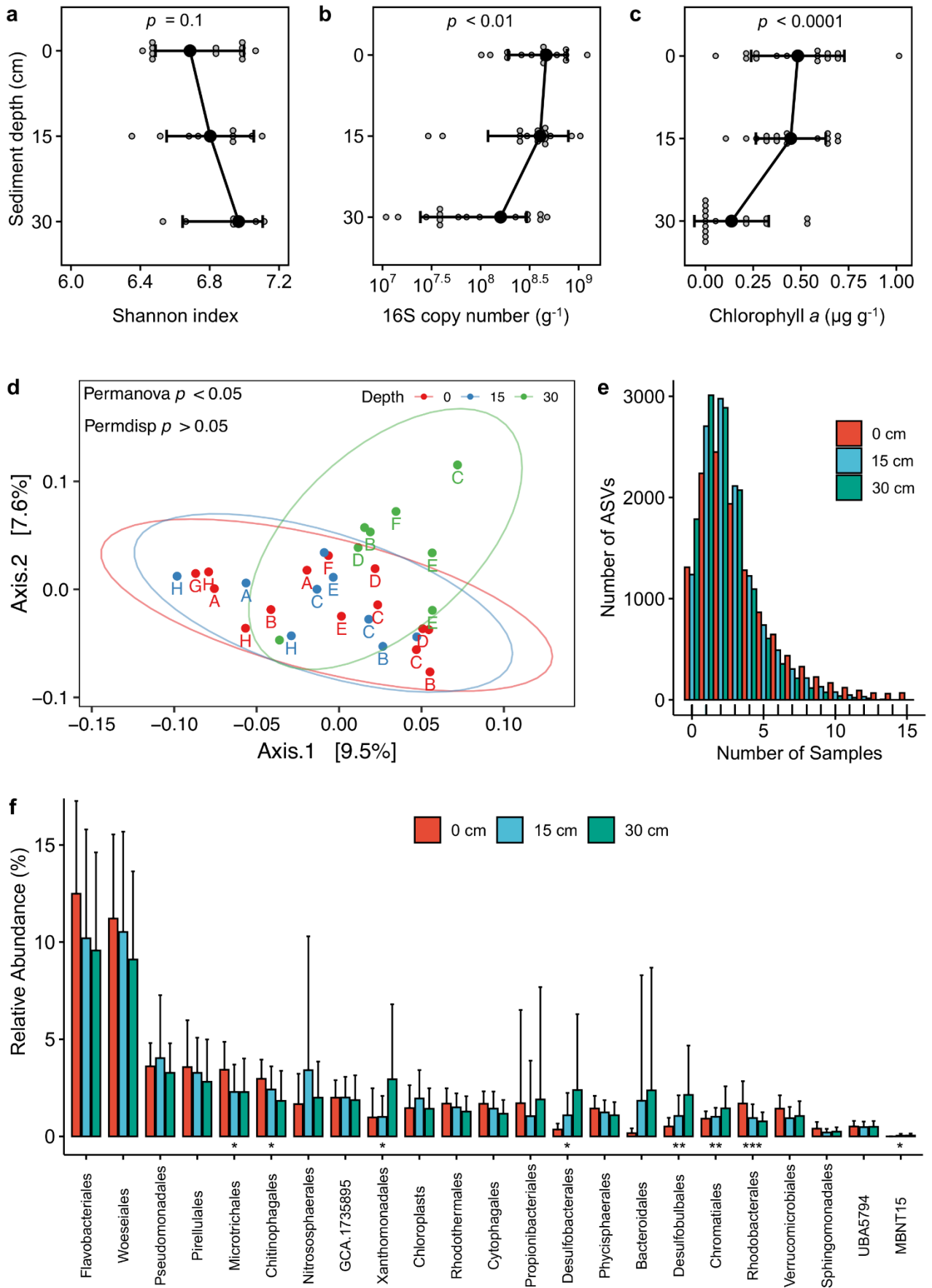
896 **Figure legends**

897

898 **Figure 1. Diversity, abundance, and composition of bacterial and archaeal**
899 **communities in permeable sediments.** The figures are based on the results of 16S
900 rRNA gene sequencing for 48 samples covering two tidal zones (intertidal, subtidal),
901 three sediment depths (0-3 cm, 13-17 cm, 27-30 cm), and eight sampling times
902 (between Oct 2016 to Oct 2017). Variations in **(a)** Shannon index (alpha diversity), **(b)**
903 16S copy number, and **(c)** chlorophyll a concentration are shown with depth; error bars
904 show standard deviations of the mean and significance was tested using one-way
905 ANOVAs. **(d)** Principal coordinates analysis (PCoA) plot visualizing pairwise
906 dissimilarity (beta diversity) of communities using weighted Unifrac. **(e)** Occupancy
907 frequency distribution of the amplicon sequence variants (ASVs) detected across the
908 samples. The histograms show the number of samples that each taxon (ASV) was
909 detected at each sediment depth. **(f)** Relative abundance of the twenty most abundant
910 orders within the sediments, as well three others represented by genome bins; error
911 bars show standard deviations of the mean and significance was tested using linear
912 regression analyses with depth treated as a continuous variable (* $p < 0.05$, ** $p <$
913 0.01).

914

915



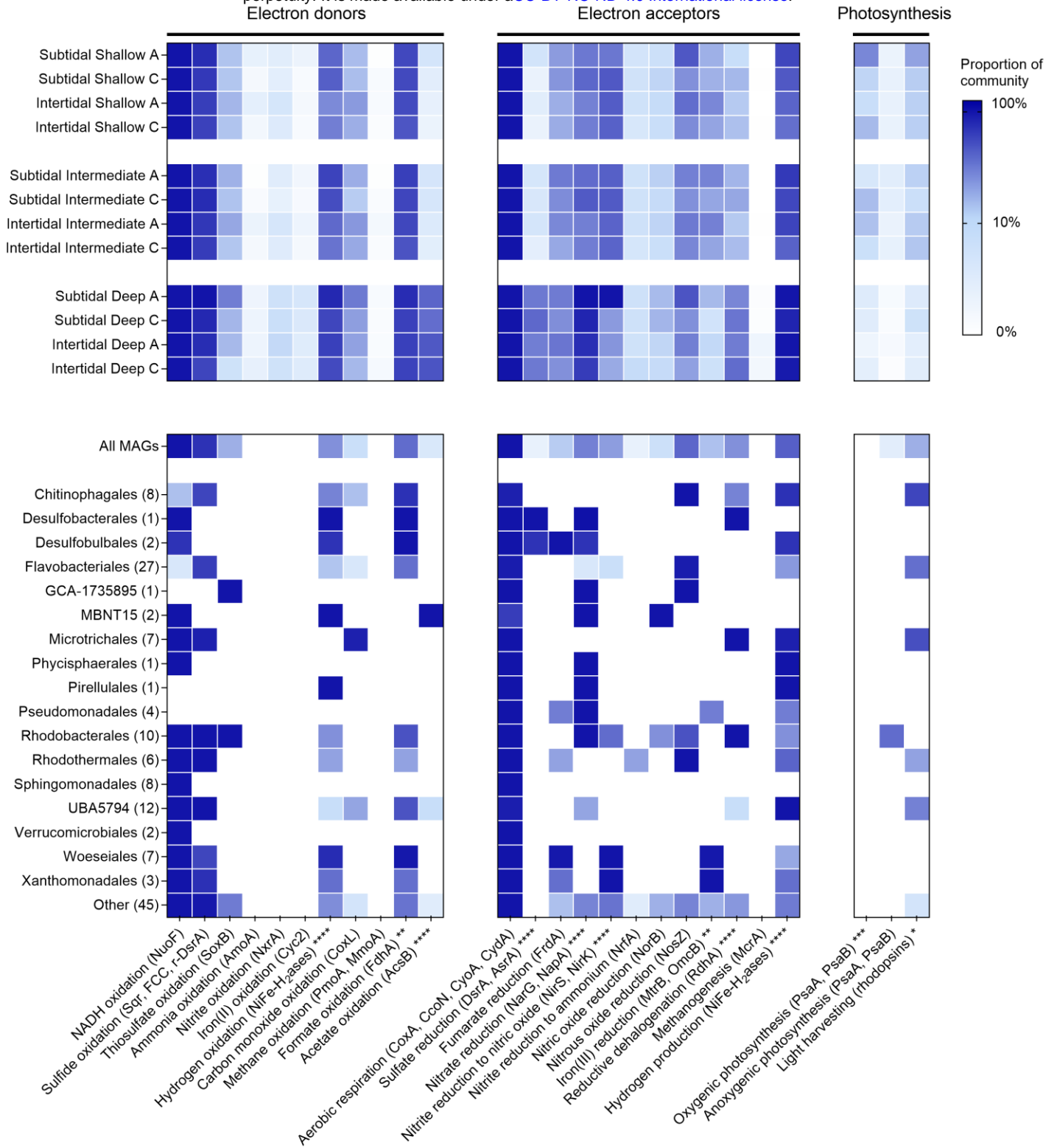
916

917

918 **Figure 2. Metabolic capacity of microbial communities in permeable sediments.**

919 Homology-based searches were used to detect key metabolic genes in 12
920 metagenomes (**Table S3**) and 147 derived metagenome-assembled genomes
921 (MAGs; **Table S6**). The upper rows show the proportion of community members in
922 each metagenome predicted to encode each gene based on the short reads; hits were
923 normalized to gene length and single-copy ribosomal marker genes. Hits were
924 summed for each process where more than one gene was searched for (up to 100%),
925 with exception of oxygenic photosynthesis where PsaA and PsbA hits were averaged
926 (reflecting both genes are required for this process to occur). The lower rows show the
927 proportion of MAGs estimated to encode each gene, with results shown by order; hits
928 are normalized based on estimated genome completeness. Metabolic marker genes
929 involved in the oxidation of electron donors and reduction of electron acceptors are
930 shown. Two-way ANOVAs were used to test whether there were significant differences
931 in relative abundance of genes between depths (* $p < 0.05$, ** $p < 0.01$, *** $p < 0.001$,
932 **** $p < 0.0001$ between shallow and deep sediments).

933



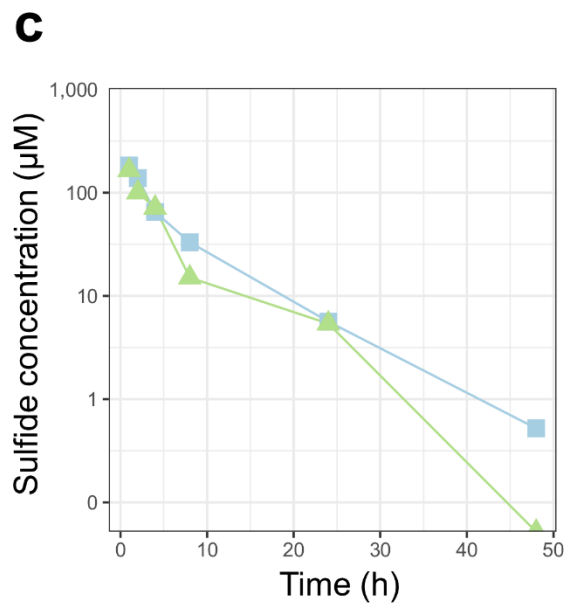
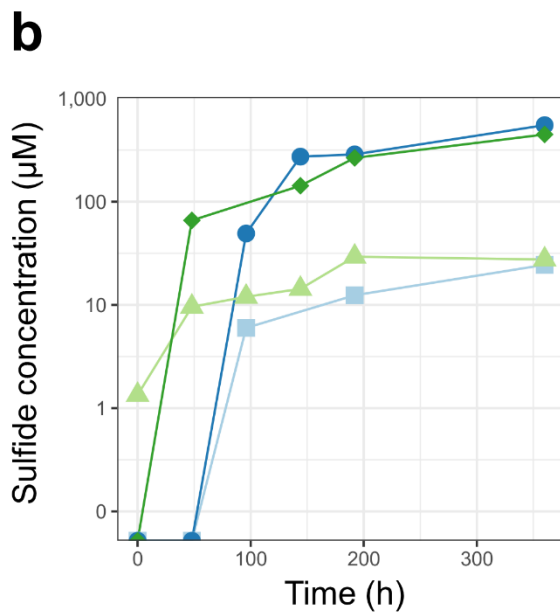
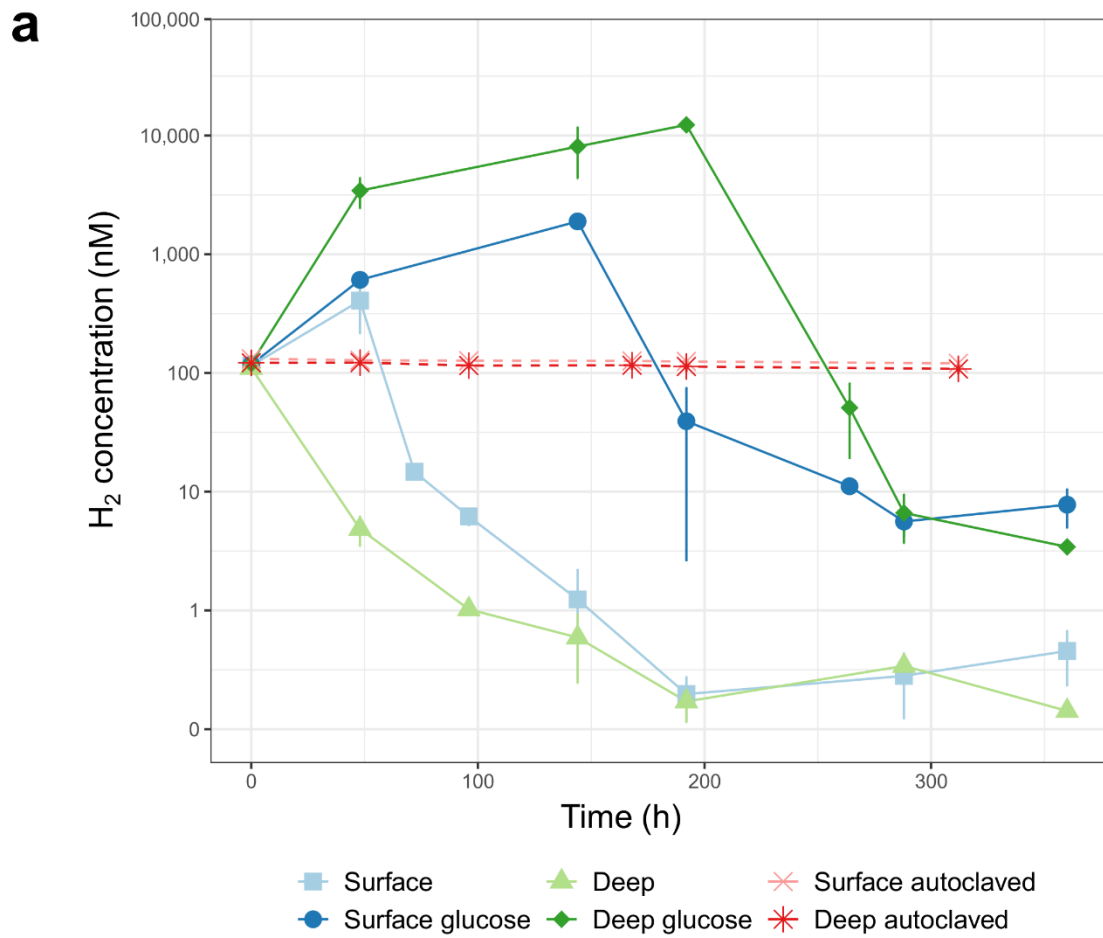
34

35

936 **Figure 3. Phylogenetic trees of genes mediating sulfur cycling.** Maximum-
937 likelihood phylogenetic trees are shown for **(a)** sulfide-quinone oxidoreductase (Sqr),
938 **(b)** flavocytochrome *c* sulfide dehydrogenase (FCC), and **(c)** dissimilatory sulfite
939 reductase A subunit (DsrA). The tree shows sequences from permeable sediment
940 metagenome-assembled genomes (colored) alongside representative reference
941 sequences (black). The trees were constructed using the JTT matrix-based model,
942 used all site, and were midpoint-rooted. Note Sqr, FCC, and the upper clade of DsrA
943 (r-DsrA; encompassing Proteobacteria bins) are known to aerobic sulfide oxidation
944 (bins colored in blue), whereas the middle clade of DsrA (encompassing
945 Desulfobacterota bins) mediate anaerobic sulfite reduction (bins colored in red). Node
946 junctions represent bootstrap support from 50 replicates. Full linear trees with
947 accession numbers are provided in **Fig. S6** (Sqr), **Fig. S7** (FCC), and **Fig. S8** (DsrA).
948

951 **Figure 4. Metabolic activities of microbial communities in sediments.** The first
952 two panels show the capacity of sands to mediate hydrogenogenic fermentation and
953 hydrogenotrophic sulfate reduction under anoxic conditions. Shallow and deep
954 sediments were incubated in nitrogen-purged slurries in the presence of 100 ppmv H₂
955 and, for spiked samples, 1 mM glucose. Changes in **(a)** H₂ concentration and **(b)**
956 sulfide concentration were measured during the experiment. For H₂ measurements,
957 error bars show standard deviations for three independent slurries. The third panel
958 shows the capacity of oxic sands to mediate sulfide oxidation. Shallow and deep
959 sediments were each incubated under oxic conditions in six independent slurries
960 amended with 200 μM Na₂S·9H₂O. Changes in **(c)** sulfide concentration were
961 measured during the timecourse, with one serum vial sacrificed per timepoint.

962



963

964

965 **Figure 5. Responses of different orders to simulated environmental disturbance.**

966 The relative abundance of microbial orders from surface (top) and deep (bottom)
967 sands is depicted with red bars. The changes of their relative abundance is shown
968 after sands were incubated in slurries for two weeks in one of three conditions:
969 continual light oxic conditions (light blue bars), continual dark anoxic conditions (green
970 bars), or disrupted conditions (dark blue bars) in which slurries were shifted between
971 light oxic and dark anoxic conditions every 24 hours. The 23 orders from **Figure 1** are
972 depicted. Error bars show standard deviations of the mean and significance was tested
973 using one-way ANOVAs (* $p < 0.05$, ** $p < 0.01$, *** $p < 0.001$, **** $p < 0.0001$). Shapes
974 next to taxon names predict habitat preferences of each order based on the obtained
975 bins: generalists (dark blue circles), oxic specialists (light blue triangles), and anoxic
976 specialists (green diamonds). Given no bins were obtained for Cytophagales,
977 Propionibacterales, Bacteroidales, Chromatiales, and chloroplasts, metabolic
978 capabilities are inferred based on cultured organisms.

979

